58916-00-105
85088-24-105

Manuscript

RECEIVED
FEB 16 1996
OSTI

November 1993

Determination of the temperature dependence of the penetration depth of Nb in Nb/AlOx/Nb Josephson junctions from a resistive measurement in a magnetic field*

D.H. Kim,[1,2] K.E. Gray,[2] J.D. Hettinger,[2] and J,H. Kang[3]

[1]*Korea Institute of Science and Technology, Seoul 130-650, Korea*

[2]*Materials Science Division*
and
Science and Technology Center for Superconductivity
Argonne National Laboratory, Argonne, IL 60439

[3]*Westinghouse Science and Technology Center, Pittsburgh, PA 15235*

jmc

*Work at KIST is supported by the Ministry of Science and Technology in Korea and the work at ANL is partially supported by the U.S. Department of Energy, Division of Basic Energy Sciences-Materials Sciences, under contract #W-31-109-ENG-38 (KEG, JDH) and the National Science Fondation-Office of Science and Technology Centers for Superconductivity contract #DMR-91-20000 (DHK).

Determination of the temperature dependence of the penetration depth of Nb in Nb/AlOx/Nb Josephson junctions from a resistive measurement in a magnetic field

D.H. Kim[1,2], K.E. Gray[2], J.D. Hettinger[2], and J.H. Kang[3]

[1] *Korea Institute of Science and Technology, Seoul 130-650, Korea*

[2] *Materials Science Division, Argonne National Laboratory, Argonne, IL 60439, USA*

[3] *Westinghouse Science and Technology Center, Pittsburgh, PA 15235, USA*

Abstract

The temperature dependence of the penetration depth of Nb films was determined from *resistive* transitions of Nb/AlO_X/Nb Josephson junctions in a constant magnetic field applied *parallel* to the junction planes. Distinct resistance peaks were observed as temperature decreases and those peaks were found to appear when the total flux threading the junction equals an integral multiple of the flux quantum. From this condition, we have determined the penetration depth at those peak positions. The temperature dependence was well described by the either dirty local limit or the two-fluid model. This method can be useful for highly fluctuating system like high-temperature superconductors.

PACS numbers: 74.30.Ci, 74.50.+r

I. Introduction

The magnetic field penetration depth λ is one of several important parameters that characterize both conventional and high-temperature superconductors. The magnitude at T = 0 as well as the temperature dependence have been studied by several methods. For instance, inductive transitions are mostly used to determine λ for needle or cylindrical shaped samples [1,2], and low-field magnetization is used for fine powders [3] and bulk materials [4]. Muon spin resonance technique [5] and polarized-neutron reflections [6] have also been used to measure λ. For thin films, kinetic inductance [7], a transmission line technique [8], and Josephson junctions [9-12] have been used to measure λ more directly.

The penetration depth of Nb has been studied extensively by many authors. We will mention only a few which are closely related to our work. Maxfield and McLean [1] measured $\lambda(T)$ of bulk Nb using inductive transition and reported that the temperature dependence was slightly deviated from BCS theory. A similar result was found by Varmazis and Strongin [2] using a tunnel diode oscillator circuit to measure inductance changes with temperature variation. For Nb films, Henkels and Kircher [8] used a transmission line technique to find out that $\lambda(T)$ followed the two-fluid model quite closely, while Broom [9] used the internal resonance of Nb Josephson junctions to measure $\lambda(T)$ which showed fair agreement with the local dirty limit.

In this work a modified Josephson junction technique has been used to determine $\lambda(T)$ of Nb films from *resistive* transitions in a magnetic field applied *parallel* to the junction plane. The standard-textbook method is to measure the magnetic-field-modulated critical current of the Josephson junction, so called "diffraction pattern" and determine λ at a corresponding temperature [12]. However, the same physical properties of this diffraction pattern can be obtained rather differently by monitoring resistance of the junction as a function of temperature in a given magnetic field. This resistive method turned out to be simple and

better than standard diffraction methods or other Josephson junction techniques [9-11] especially near T_c where thermal fluctuations are strong.

II. Theoretical Background

For a rectangular junction with uniform current flow across the junction, the maximum supercurrent is given as

$$I_{max} = I_0 \left| \frac{\sin(\pi\Phi / \Phi_0)}{\pi\Phi / \Phi_0} \right| \qquad (1),$$

where Φ is the total flux threading the junction and $\Phi_0 = 2.07 \times 10^{-7}$ gauss-cm^2 is a flux quantum. When Φ is an integral multiple of Φ_0, the supercurrent through the junction vanishes, and this condition enables the determination of λ. For sufficiently thick electrodes, $\Phi = \mu_0 H w(\lambda_1+\lambda_2+d)$, where w is the junction width facing the uniform magnetic field H, d is the thickness of the insulating barrier, and λ_1 and λ_2 are the penetration depths for base and counter electrodes, respectively. For a general case of electrodes of finite thicknesses, the field penetration from the both sides of the films should be considered. Thus, Φ is given by London local theory as [8]

$$\Phi = \mu_0 H w \left[d + \lambda_1 \tanh\left(\frac{b_1}{2\lambda_1}\right) + \lambda_2 \tanh\left(\frac{b_2}{2\lambda_2}\right) \right]$$
$$\equiv \mu_0 H w h_{eff} \qquad (2),$$

where h_{eff} is the effective depth of field penetration, and b_1 and b_2 are the thicknesses of two electrodes, respectively. In the present work, Nb is used for both electrodes, so $\lambda_1 = \lambda_2 = \lambda$. The conventional method to measure the diffraction pattern of I_{max}, Eq. 1, is to vary magnetic field at a fixed T.

In the case of a constant-current-driven junction, the transport current is first carried by superelectrons. However, when $\Phi = N\Phi_0$ where N is a nonzero integer, $I_{max} = 0$, thus the bias current should flow via quasiparticle tunneling. Since this quasiparticle channel is

dissipative, resistance appears across the junction. Suppose that we change the temperature of the junction in a given H, Φ will change continuously with T due to the temperature dependence of the penetration depth. Therefore, the condition that $\Phi = N\Phi_0$ will be satisfied for at least one temperature because λ diverges as T approaches T_c. Now we define the temperatures where $\Phi = N\Phi_0$ as T_{pN}. At T_{pN}, the resistance across the junction will appear, while showing zero or possibly a small resistance due to thermal noise [13] at other T $< T_c$. Therefore, distinct resistance peaks will show up at T_{pN}, and by solving Eq. 2, $\lambda(T_{pN})$ can be obtained. As a magnetic field is varied, the locations of resistance peaks will move to different temperatures. By doing so, the temperature dependence as well as the magnitude of the penetration depth can be determined for $T < T_c$. A method to determine the parameter N will be described later.

III. Experiment and Results

The Nb films were sputter deposited in a system with a load-lock chamber. The substrate was a 2-inch silicon wafer with 200-nm SiO_2 on the surface. The background pressure of the system was maintained at ~ 10^{-9} torr. During film deposition, the substrates were kept in contact with a water-cooled copper plate. The Nb junctions were fabricated on such Nb films using an AlO_x barrier, which was formed by exposing a 7.5-nm thick Al layer to 150 mtorr of pure oxygen gas for 30 min. Junction areas were defined by the selective niobium etching process (SNEP), which uses reactive ion etching and anodization of Nb. We studied two junctions, K19 (16 x 16 μm^2) and K51 (8 x 12 μm^2). The physical properties of the junctions and the Nb electrodes are listed in Table 1.

We determined $\lambda(T)$ of Nb films from the resistive transitions of Nb/AlO_x/Nb Josephson junctions in a constant magnetic field applied *parallel* to the junction planes. Resistances were measured using a standard four-terminal, ac lock-in technique. Typical bias currents were less than 2 μA. The measurements of the Nb electrode in perpendicular fields showed much larger $H_{c2}(T)$ than that of pure Nb. From this, H_{c1} at T=0 can be estimated from the

dirty limit formula to be ~ 230 gauss. All measurements were done in a parallel magnetic field of less than 60 gauss to assure the Meissner state of the Nb films over most of the temperature range. In a *perpendicular* field, field penetration occurs at even smaller fields and in this case it was found that Josephson coupling energy depends on field as 1/H [14].

Typical resistive transitions of the K19 junction are shown in Fig. 1 for parallel magnetic fields of 22.3 and 23.6 gauss. Those of the K51 junction showed almost identical behavior. The initial drop to ~ 0.3 Ω is due to the sharp transition of the electrodes. The resistance peaks are clearly visible. As mentioned before, the peaks appear when the junction resistance returns to the quasiparticle resistance of the junction due to $I_{max}(T_{pN}) = 0$. Note that slight variations of the magnetic field induce a clear shift of T_{pN}. Between the peaks, the junction goes superconducting for $T < 8.5$ K implying that $I_{max}(T)$ is larger than the bias current. However, for $T > 8.5$ K, small $I_{max}(T)$ and thermal noise in the junction seem to be responsible for the finite resistance and the smearing of peaks of higher N. Here we took only clear peaks to obtain $\lambda(T)$.

Since there is no independent way to determine the integer N, diffraction patterns of I_{max} were measured at 4.2K. It served as a reference point to get the correct N. Critical current variation with magnetic field of K19 is shown in Fig. 2. Also shown as a solid line is the fit to Eq. 1. The overall pattern follows Eq. 1 pretty well. However, we found that the first few minima of I_{max} at integral flux quantum penetration were not exactly zero. This is an indication of slightly nonuniform current flow. The Josephson penetration depth λ_J estimated by [15]

$$\lambda_J = \left[\frac{\hbar}{2e\mu_0 h_{eff}}\right]^{1/2} \qquad (3)$$

was 8.2 μm at 4.2 K about half of the width of the junction (16 μm), thus barely satisfying the small junction limit. From field values at which I_{max} are the local minima and using Eq. 2 with appropriate electrode thicknesses, $\lambda(4.2K) = 87.8 \pm 2$ nm was obtained. The error is

mostly due to the uncertainty in the electrode thickness measurement. Similarly, $\lambda(4.2K)$ = 62.9±2 nm was obtained from the diffraction pattern of K51. In the case of K51, Josephson penetration turned out to be 11 μm, almost twice the half-width of the junction.

For a given H, calculated $\lambda(T)$ depends on N. The peak at 7.18 K of the 23.6 gauss data corresponds to λ = 22.7, 49.8, 80.7, 121, 179, and 296 nm for N = 1, 2, 3, 4, 5, and 6, respectively, from solving Eq. 2. Since $\lambda(4.2\ K)$ is determined as 87.8 nm by diffraction pattern, $\lambda(7.18\ K)$ should be greater than 87.8 nm, thus the first available value is 121 nm for N = 4. Therefore, peaks with N from 1 to 3 would not appear for $4.2\ K < T < 7.18\ K$. Consequently the peaks at 8.4 and 8.9 K correspond to N = 5 (179 nm) and N = 6 (296 nm), respectively. The temperature interval between adjacent peaks gets smaller as T increases due to the steep increase of λ. Similarly, the peaks in the 22.3 gauss data at 7.79 and 8.57 K corresponds to N = 4 (132 nm) and N = 5 (204 nm), respectively. The data of $\lambda(T)$ obtained at five different fields for the K19 junction are gathered and shown in Fig. 3(a). The same procedure can be applied to the K51 junction. Since the shape of K51 is rectangular, two sets of $\lambda(T)$ were determined, one for magnetic field facing the 8 μm side and the other for the field facing the 12 μm side. As shown in Fig. 3(b), both data sets agree with each other very well.

The resistance peaks were not detected below 7 K for the K19 junction and 6 K for the K51 junction even in an appropriate magnetic field which predict resistance peaks in such tenperature regions. It is presumably because $I_{max}(T_{pN})$ was greater than the bias current due to the nonuniform current flow as mentioned before. At higher temperatures $I_{max}(T_{pN})$ becomes smaller than the bias current, so the resistance peaks appear.

We were able to identify the resistance peaks up to $T/T_c = 0.96$. This temperature range is at least the same or better than other Josephson junction techniques [9-11]. For instance, the standard diffraction method near T_c requires an extensive fitting procedure to a given model due to the thermal rounding of current-voltage characteristics. This resistive method is

simple and provides quantitative results directly. The inductive transition [2] and transmission methods [8] have shown the similar temperature ranges.

IV. Discussion

Maxfield and McLean [1] measured $\lambda(T)$ of pure Nb bulk of the resistivity ratio of $R_{300}/R_{4.2} = 115$. They obtained the penetration depth at T =0, $\lambda(0) = .47\pm5$ nm and the London penetration depth $\lambda_L(0) = 39\pm5$ nm. The BCS coherence length ξ_0 was estimated to be 38 nm with a mean free path $l = 400$ nm at T = 0. Since $\xi_0 = \hbar v_F / \pi\Delta(0)$, where Δ is the gap energy, and $\lambda_L(0)$ are rather insensitive to the details of the sample, we assumed that ξ_0 and $\lambda_L(0)$ of Nb films are the same as those of bulk Nb, i.e., $\xi_0 = 38$ nm and $\lambda_L(0)= 39$ nm. In our junctions, $\Delta(4.2K) = 1.2$ meV was obtained which corresponds to $2\Delta(0) = 3.13\ k_B T_c$. Varmazis and Strongin [2] reported slightly different values of $\lambda_L(0) = 31.5\pm1.5$ nm and $\xi_0 =$ 35.6 nm from kinetic inductance measurement of bulk Nb.

Since $\lambda_L/\xi_0 \approx 1$, the London local approximation is better than the extreme anomalous limit where $\lambda_L/\xi_0 \approx 0$ [15]. Note that we already used the London theory in deriving Eq. 2 to obtain $\lambda(T)$. In the local approximation, the penetration depth is related to the mean free path by [15]

$$\lambda(T) = \lambda_L(T)\left[1+\frac{\xi_0}{J(0,T)\ell}\right]^{1/2} \qquad (4)$$

where J(0,T) is the BCS range function which varies from 1 at T = 0 to 1.33 at T= T_c. In the dirty local limit ($l << \xi_0$), Eq. 4 reduces to [15]

$$\lambda(T) = \lambda_L(T)\left[\frac{\xi_0}{J(0,T)\ell}\right]^{1/2} \qquad (5)$$

$$= \lambda(0)\left[\frac{\Delta(T)}{\Delta(0)}\tanh\left(\frac{\Delta(T)}{2k_BT}\right)\right]^{-1/2} \qquad (6)$$

On the other hand, the empirical two-fluid approximation is given by

$$\lambda(T) = \lambda(0)\left[1-\left(\frac{T}{T_c}\right)^4\right]^{-1/2} \qquad (7).$$

The results of the two approximations are shown in Fig. 3 as solid lines for the dirty local limit (Eq. 6) and dotted lines for the two-fluid approximation (Eq. 7). We forced both lines to include the data point at 4.2 K. For K19, the dirty local limit provides an excellent fit over the full temperature range, while, for K51, the dirty local limit behavior is a better fit at low temperatures while the two-fluid model is better near T_c. Zero-temperature penetration depths were determined as 84.4±2 nm and 60.9±2 nm for K19 and K51, respectively, in the dirty local limit approximation.

The value of λ(4.2K) = 86 nm was reported for 235-nm thick Nb films measured by a transmission line technique [7]. Broom [9] showed that λ(4.2K) varied from 86 to 100 nm, and Cucolo [12] reported 88 and 89 nm from the standard diffraction pattern of a Nb-Pb junction. Those values of λ(4.2K) measured using thin films are in good agreement with the result of K19. On the other hand, we found smaller value of λ(4.2K) = 63 nm from K51. Overall, effective penetration depths of thin films are much larger than those of bulk ones. Such a variation of λ among samples could originate from the different characteristics of the metal-insulator interfaces. For instance, there may not be a sharp interface between the oxide barrier and the metal electrodes, or in the present case, all of the aluminum deposited may not be completely oxidized in the insulating barrier, thus leaving some normal layer. As pointed out by Varmazis and Strongin [2], the effective penetration depth is very sensitive to the nature of the surface. They calculated the effective penetration depth as a function of the ratio of coherence length to the inverse of logarithmic slope of order parameter at the boundary. As the ratio increases, i.e., the nature of boundary deviates from ideal metal-vacuum interface, the effective penetration depth increases. They also confirmed that careful surface preparation was necessary for the accurate measurement of the penetration depth.

Another possible reason especially for the junction samples would be unequal penetration depths in the two Nb electrodes as suggested by Broom [9].

Mean free paths at T = 0 can be determined from Eq. 4 or 5 using $\lambda_L(0) = 39$ nm. We obtained $l(0) \approx 8.1$ nm for K19 and $l(0) \approx 16$ nm for K51, indeed much smaller than the bulk value of $l(0) = 400$ nm. The short mean free paths could be an indication of surface properties or the polycrystallinity of the sample because the electrodes were deposited at cooling-water temperature. Whatever the origin, they are consistent with the small resistivity ratios (see Table 1). The magnitude of $l(0)$ of K19 is even shorter than that of K51. This gives a possible explanation why the dirty local limit is a good fit for K19 since the condition ($l << \xi_0$) is well satisfied.

When the junction resistance returns to quasiparticle resistance Rq, the magnitude should increase as temperature decreases since $Rq \sim \exp(-\Delta(T)/k_BT)$. Instead, almost temperature-independent peak-resistances were observed (Fig. 1). This is possibly due to the nonuniform current flow across the junction as evidenced by the fact that the first few minima of I_{max} at integral flux quantum penetration are not exactly zero as shown in Fig. 2. Note that peak resistance of ~ 0.3 Ω is very close to the junction resistance of 0.28 Ω determined from IV characteristics at 4.2 K.

V. Summary

We have measured the resistive transitions of $Nb/AlO_x/Nb$ Josephson junctions in a constant magnetic field applied *parallel* to the junction planes. The measured resistance returned to the quasiparticle resistance when the total flux threading the junction equaled an integral multiple of the flux quantum. From this condition, we have the determined temperature dependence of the penetration depth of Nb films. The results obtained from this unusual method were well described by either the dirty local limit or the two-fluid model. This method is rather insensitive to thermal fluctuations when compared to the standard

diffraction method, thus it could be useful in determination of $\lambda(T)$ for highly fluctuating system like high-temperature superconductors.

Acknowledgments

The work at KIST is supported by the Ministry of Science and Technology in Korea, and the work at ANL is partially supported by the U.S. Department of Energy, Basic Energy Sciences-Materials Sciences, under contract #W-31-109-ENG-38 (KEG, JDH) and NSF Office of Science and Technology under contract DMR 91-2000 (DHK).

References

1. B.W. Maxfield and W.L. McLean, Phys. Rev. **139**, 1515 (1965).

2. C. Varmazis and M. Strongin, Phys. Rev. **B10**, 1885 (1974).

3. J.R. Cooper, C.T. Chu, L.W. Zhou, B. Dunn, and G. Gruner, Phys. Rev. **B37**, 638 (1988).

4. L. Kresin-Elbaum, R.L. Greene, F. Holtzburg, A.P. Malozemoff, and Y. Yeshurun, Phys. Rev. Lett. **62**, 217 (1989).

5. D.R. Harshman, G. Aeppli, E.J. Ansaldo, B. Batlogg, J.H. Brewer, J.F. Carolan, R.J. Cava, and M. Celio, Phys. Rev. **B36**, 2386 (1987).

6. G.P. Felcher, R.T. Kampwirth, K.E. Gray, and R. Felici, Phys. Rev. Lett. **52**, 1539 (1984).

7. R. Merservey and P.M. Tedrow, J. Appl. Phys. **40**, 2028 (1969); J.D. Lejeune and D.G. Naugle, J. Low. Temp. Phys. **22**, 425 (1976).

8. W.H. Henkels and C.J. Kircher, IEEE Trans. Magn. **13**, 63 (1977).

9. R.F. Broom, J. Appl. Phys. **47**, 5432 (1976).

10. G.E. Peabody and R. Merservey, Phys. Rev. **B6**, 2579 (1972).

11. F. Dettman and R. Rexhauser, Phys. Status Solidi **A51**, 197 (1978); D.S. Pyun, E.R. Ulm, and T.R. Lemberger, Phys. Rev. **B39**, 4140 (1989).

12. A.M. Cucolo, S. Pace, R. Vaglio, A. di Chiara, G. Peluso, and M. Ruso, J. Low Temp. Phys. **50**, 301 (1983).

13. V. Ambegaokar and B.I. Halperin, Phys. Rev. Lett. **22**, 1364 (1969).

14. D.H. Kim, K.E. Gray, and J.H. Kang, Phys. Rev. **B45**, 7563 (1992).

15. M. Tinkham, *Introduction to Superconductivity*, New York, McGraw-Hill, 1975.

Figure Caption

Fig. 1, The resistive transitions of the K19 junction are shown for fields of 22.3 (solid square) and 23.6 gauss (open square) applied parallel to the junction plane. The peaks appear when the total flux threading the junction is an integral multiple of the flux quantum.

Fig. 2, The variation of the critical current of the K19 junction with magnetic field measured at 4.2 K is shown. Solid line is a fit to Eq. 1.

Fig. 3, Penetration depths of Nb films of K19 (a) and K51 (b) junctions as a function of temperature. Solid lines are fits to the dirty local limit (Eq. 6) and dotted lines are fits to the two-fluid model (Eq. 7). Two sets of $\lambda(T)$ in Fig. 3(b) are for magnetic fields facing the 8 μm (solid square) and the 12 μm side (open square), respectively.

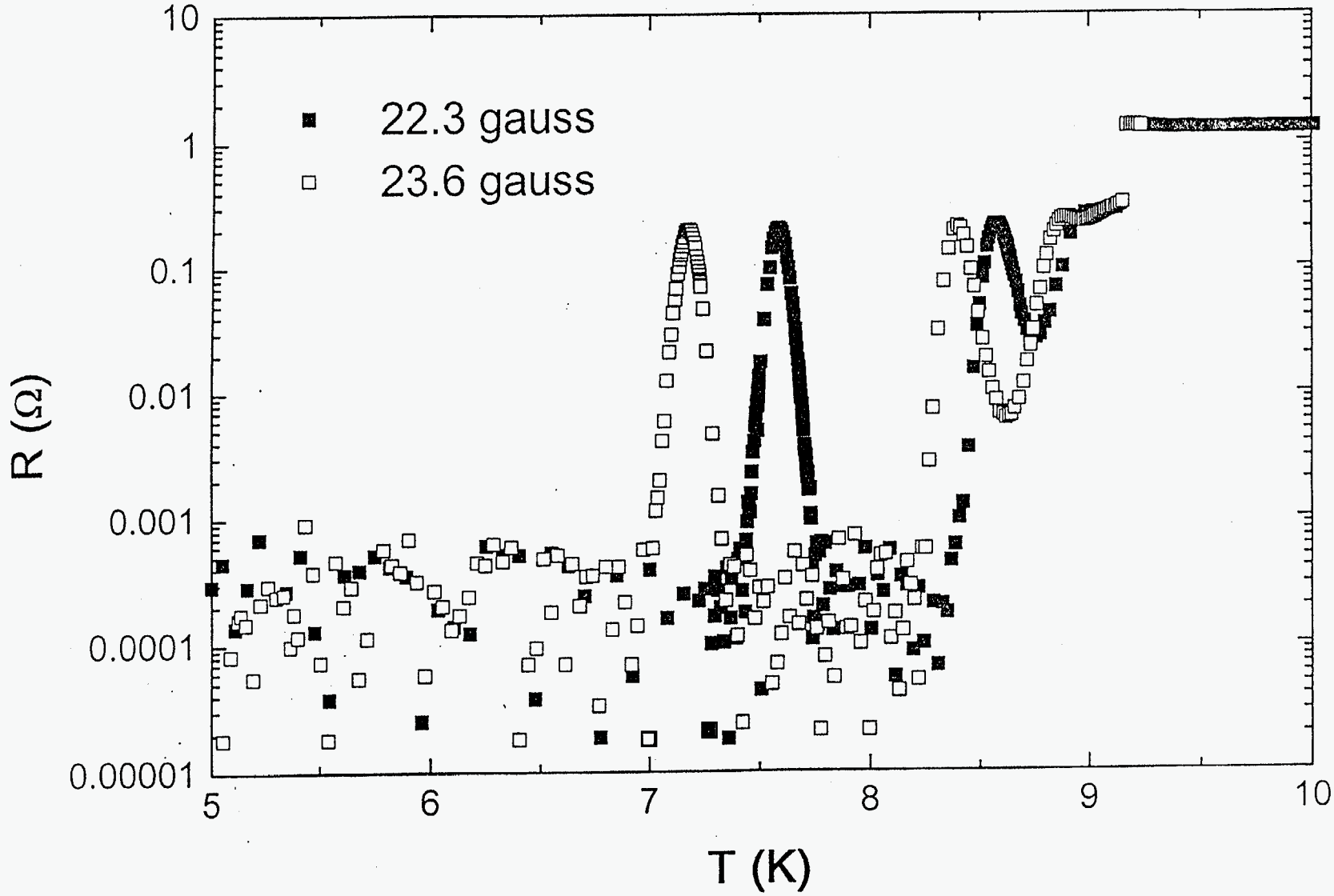
22.3 gauss
23.6 gauss
R (Ω)
T (K)
10
1
0.1
0.01
0.001
0.0001
0.00001
5
6
7
8
9
10

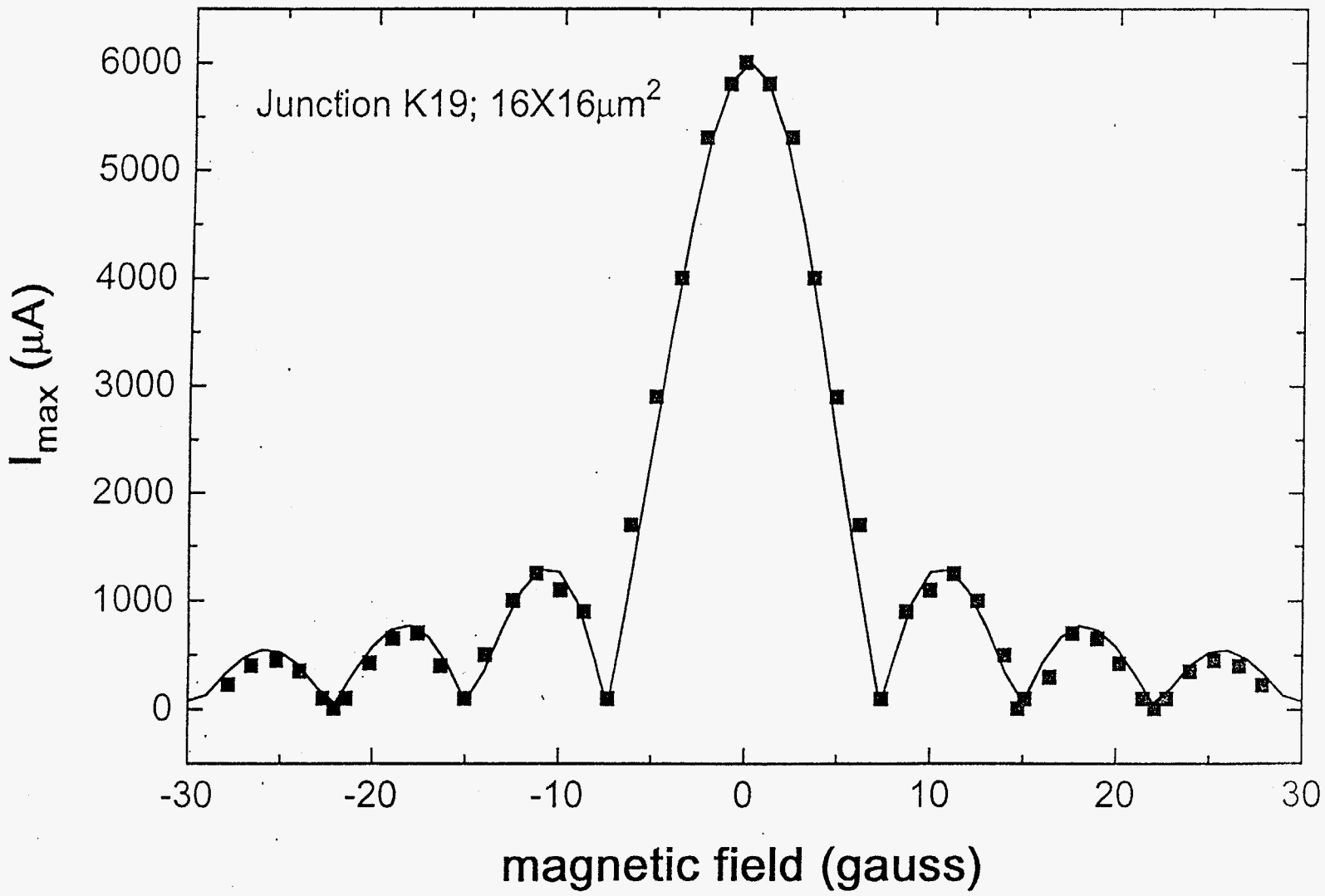
Junction K19; 16X16μm²
6000
5000
4000
3000
2000
1000
0
I_max (μA)
-30
-20
-10
0
10
20
30
magnetic field (gauss)

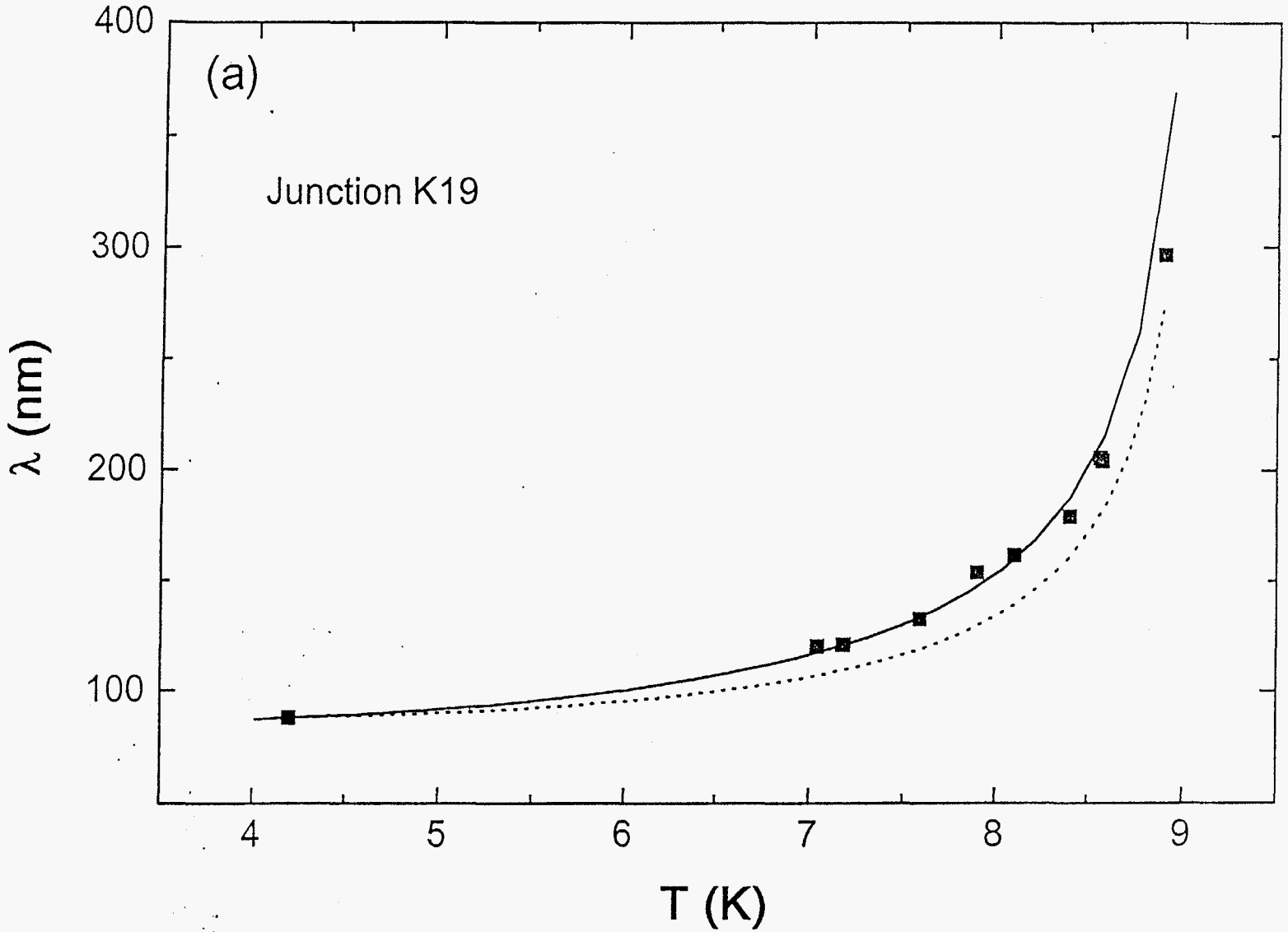
(a)
Junction K19
400
300
200
100
λ (nm)
4
5
6
7
8
9
T (K)

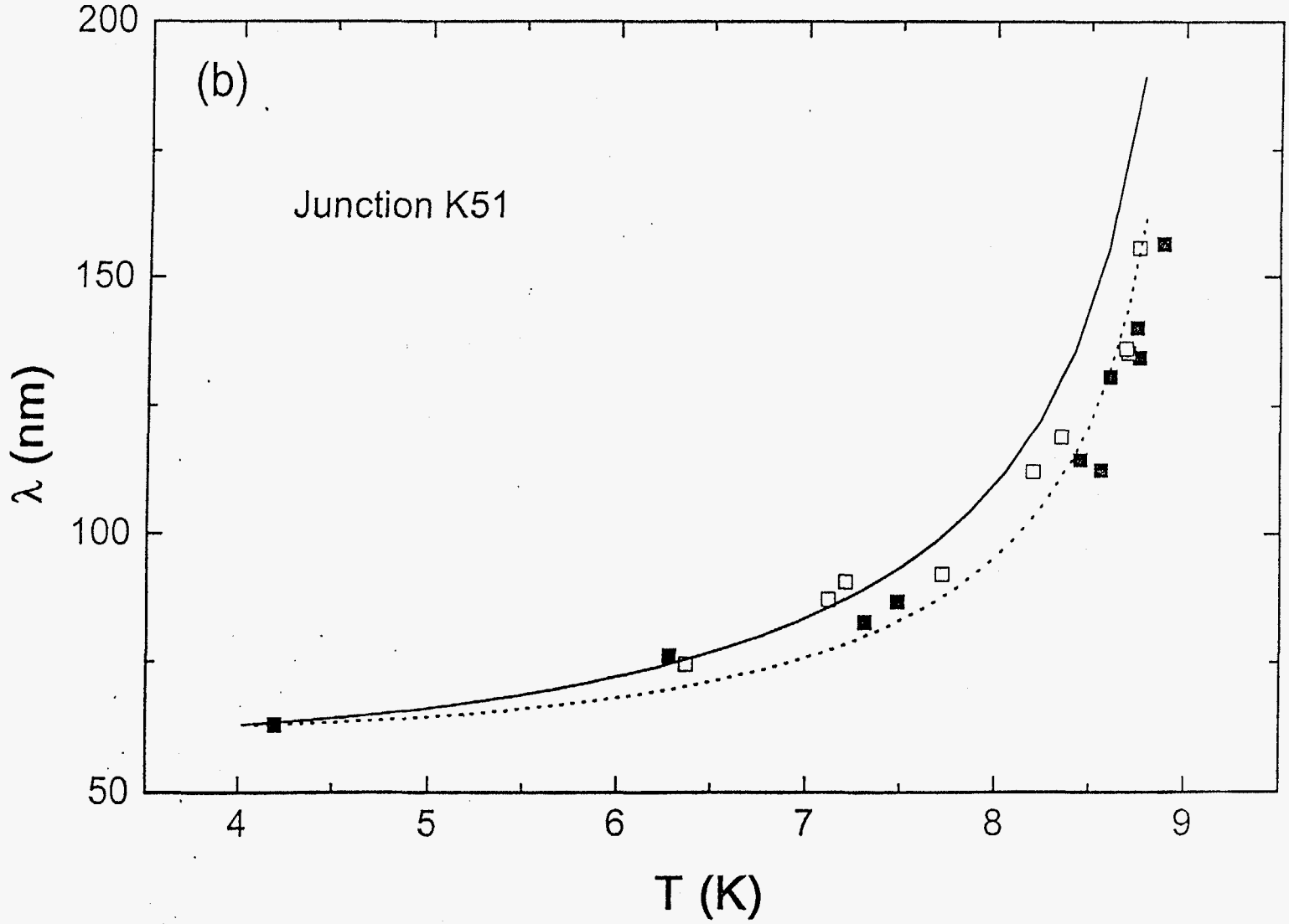
(b)
Junction K51
200
150
100
50
λ (nm)
4
5
6
7
8
9
T (K)

Table 1. Physical properties of the junctions and electrodes are listed.

sample	size	J_c at 4.2 K	R_N at 4.2 K	λ_J at 4.2 K	T_c	$R_{300}/R_{4.2}$ of Nb	Δ at 4.2 K	thicknesses of base and counter electrodes	λ at 4.2 K
	(μm^2)	(A/cm^2)	(Ω)	(μm)	(K)		(meV)	(nm)	(nm)
K19	16 x 16	1560	0.28	8.2	9.13	4.9	1.4	222±10, 502±10	87.8±2
K51	8 x 12	2190	1.0	11	9.15	8.5	1.4	185±10, 502±10	62.9±2